ACS APPLIED MATERIALS & INTERFACES

Research Article

www.acsami.org

Neat C_{70}-Based Bulk-Heterojunction Polymer Solar Cells with Excellent Acceptor Dispersion

Nicola Gasparini,[†] Sara Righi,[‡] Francesca Tinti,[†] Alberto Savoini,[§] Alessandra Cominetti,[§] Riccardo Po,*[,†,§] and Nadia Camaioni*[,†]

[†]Istituto per la Sintesi Organica e la Fotoreattività, Consiglio Nazionale delle Ricerche, via P. Gobetti 101, I-40129 Bologna, Italy

[‡]Laboratorio di Micro e Submicro Tecnologie Abilitanti per l'Emilia Romagna (MIST E-R S.C.R.L.), via P. Gobetti 101, I-40129 Bologna, Italy

[§]Research Center for Renewable Energies & Environment, Istituto ENI Donegani, ENI S.p.A., via Fauser 4, I-28100 Novara, Italy

Supporting Information

ABSTRACT: The replacement of common fullerene derivatives with neat-C_{70} could be an effective approach to restrain the costs of organic photovoltaics and increase their sustainability. In this study, bulk-heterojunction solar cells made of neat-C_{70} and low energy-gap conjugated polymers, PTB7 and PCDTBT, are thoroughly investigated and compared. Upon replacing $PC_{70}BM$ with C_{70}, the mobility of positive carriers in the donor phase is roughly reduced by 1 order of magnitude, while that of electrons is only slightly modified. It is shown that the main loss mechanism of the investigated neat-C_{70} solar cells is a low mobility-lifetime product. Nevertheless, PCDTBT:C_{70} devices undergo a limited loss of 7.5%, compared to the reference PCDTBT:$PC_{70}BM$ cells, reaching a record efficiency (4.44%) for polymer solar cells with unfunctionalized fullerenes. The moderate efficiency loss of PCDTBT:C_{70} devices, due to an unexpected excellent miscibility of PCDTBT:C_{70} blends, demonstrates that efficient solar cells made of neat-fullerene are possible. The efficient dispersion of C_{70} in the PCDTBT matrix is attributed to an interaction between fullerene and the carbazole unit of the polymer.

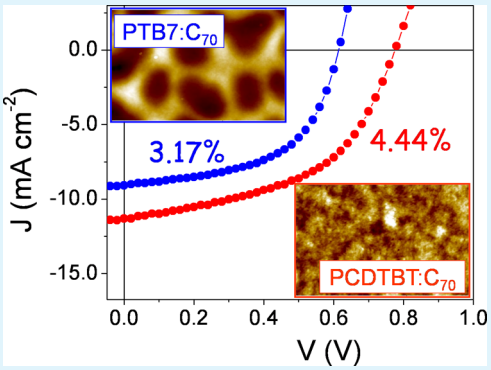

KEYWORDS: *organic solar cells, conjugated polymers, carbazole, fullerene, neat C_{70}*

1. INTRODUCTION

Thin-film solar cells made of solution-processable organic materials are regarded as a potential low-cost photovoltaic technology. Outstanding power conversion efficiencies (PCEs) have been reached in recent years for organic solar cells based on an interpenetrated network between an electron-donor and an electron-acceptor material (the so-called bulk-heterojunction, BHJ, structure).[1−4] The rapid enhancement of efficiency has been primarily achieved through the development of improved donor materials,[5−9] in addition to the fine control of the blend morphology[10] and the optimization of device architecture.[11,12] On the other hand, soluble derivatives of fullerenes have become the dominant acceptor materials,[13−15] due to their outstanding properties including a high mobility of negative charge carriers.[16,17] Currently, the 20 top-performing polymer donors give their best when combined with [6,6]-phenyl C_{71}-butyric acid methylester ($PC_{70}BM$), resulting in a power conversion efficiency of over 7.5% for the related solar cells.[18] Small-molecules acceptors have been also used, but in general, their performances are still inferior compared to fullerenes.[13]

As mentioned before, the most attractive feature of organic solar cells is the promise of a significantly lower cost compared to conventional inorganic photovoltaic technologies. This is because of solution processing and compatibility with flexible substrates, enabling the manufacturing at low temperatures and in a continuous high-throughput printing process.[19,20] Recently, it has been reported that, in an industrial scenario, the processing costs of organic solar cells are negligible in comparison to the material costs,[21] which are dependent on the synthetic complexity of the organic compounds.[18,22−24] In this frame, the use of unfunctionalized fullerenes would be extremely advantageous, thanks to their availability and relatively low cost. Indeed, the cost of neat C_{70} is currently roughly one-fifth of that of the widely employed $PC_{70}BM$.[25] Compared to the readily soluble $PC_{70}BM$, a further advantage of neat C_{70} is its higher molar extinction coefficient in the 350−650 nm wavelength region,[26] which improves the light absorption of the active layer.

In addition, fullerene acceptors are the most energy−intensive materials used in organic solar cells manufacturing, as demonstrated by a recently published analysis on the

Received: September 18, 2014
Accepted: October 27, 2014
Published: October 27, 2014

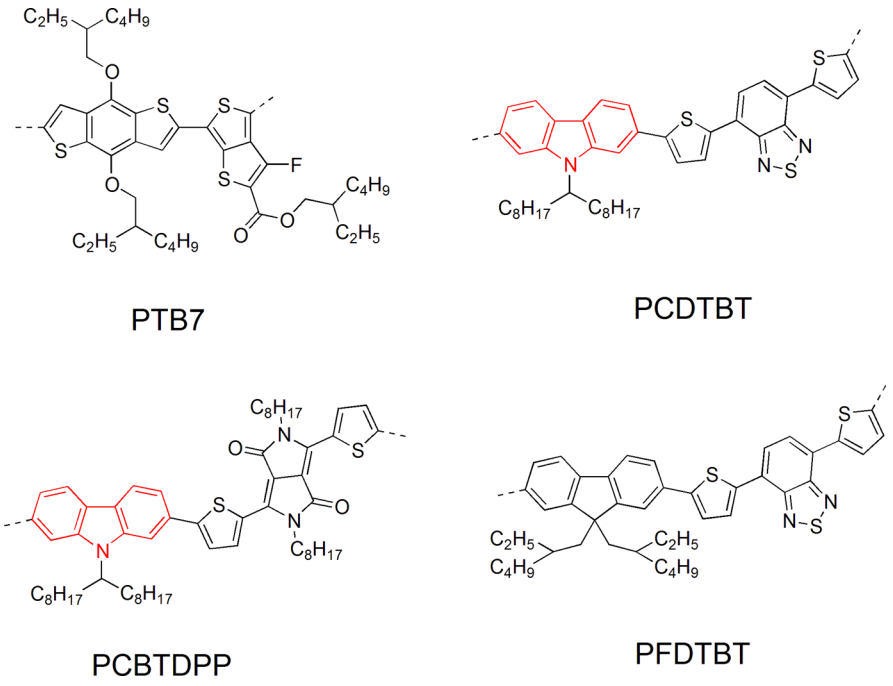

Figure 1. Monomer structure of the polymers used in this study.

cumulative energy demand (CED) of OPV.[27] In particular, the embodied energy of functional fullerenes ranges from about 85 to 125 GJ/kg and is 123 GJ/kg for $PC_{70}BM$. Thus, to further improve the sustainability of the OPV technology, which on the other hand is already a pretty sustainable energy technology, the investigation of alternatives to PCBM and $PC_{70}BM$ is very important. From this point of view, the use of unfunctionalized fullerenes might represent a step forward, since the embodied energies of C_{60} and C_{70} are 35 and 54 GJ/kg, respectively.[27]

C_{60} and C_{70} acceptors have been seldom used in the fabrication of BHJ solar cells, because of their low solubility which causes aggregation and poor film morphology.[28,29] The published studies on BHJ polymer solar cells based on neat fullerenes as acceptors are scarce. Most of them have been carried out on P3HT:C_{60} devices (P3HT is regioregular poly(3-hexylthiophene)),[30,31] with best efficiencies ranging between 2.2 and 2.6%, achieved through the appropriate choice of the solvent,[32,33] or by using interfacial agents,[34] or by applying a vapor solvent treament.[35] Despite its light absorption ability, neat C_{70} has been poorly investigated as acceptor component in polymer solar cells. An efficiency of 1.47% has been reported for P3HT:C_{70} solar cells,[36,37] while an interesting 3.05% has been achieved for PTB7:C_{70} blends (PTB7 is poly({4,8-bis[(2-ethylhexyl)oxy]benzo[1,2-b:4,5-b′]dithiophene-2,6-diyl}{3-fluoro-2-[(2-ethylhexyl)carbonyl]thieno[3,4-*b*]thiophenediyl})) deposited from 1,2,4-trimethylbenzene,[38] that has been recently further increased to more than 4% by using a polyelectrolyte buffer layer.[39]

In this study, BHJ solar cells made of C_{70} and two low bandgap electron-donors, PTB7 and PCDTBT (PCDTBT is poly[N-9′-heptadecanyl-2,7-carbazole-*alt*-5,5-(4′,7′-di-2-thienyl-2′,1′,3′-benzothiadiazole)]) are investigated and compared, in order to explore both the opportunities and the limitations in the use of unfunctionalized C_{70} as electron-acceptor. It is shown that an unexpected and excellent miscibility between the donor and the acceptor component is achieved in the case of PCDTBT:C_{70} blends, resulting in limited losses for the related solar cells. The observed excellent miscibility has been never observed for blends between conjugated polymers and neat fullerenes and is attributed to the carbazole unit of the polymer.

2. EXPERIMENTAL SECTION

Materials. PCDTBT was purchased from 1-Material Inc., PTB7 and PCBTDPP from Luminescence Technology Corp., $PC_{70}BM$ and C_{70} from Sigma-Aldrich. All materials were used as received. PFDTBT was synthesized through Suzuki polycondensation following a previously reported procedure.[40]

Devices Fabrication. Solar cells were fabricated onto patterned ITO-coated glass substrates (Kintec, sheet resistance of 20 Ω/□), previously cleaned in detergent and water, and then ultrasonicated in acetone and isopropyl alcohol for 15 min each. Prior the deposition of the active layers, a 40 nm tick layer of poly(3,4-ethylenedioxythiophene)poly(styrenesulfonate) (PEDOT:PSS) (Clevios P VP AI 4083) was spin-coated at 4000 rpm onto UV-ozone-treated substrates, then baked in an oven at 140 °C for 10 min. The active layers were spin-coated in air onto the ITO/PEDOT:PSS substrates. For PTB7:$PC_{70}BM$ and PCDTBT:$PC_{70}BM$ reference devices, optimized procedures were used: the PTB7:$PC_{70}BM$ active layer was dissolved in mixed chlorobenzene/1,8-diiodoctane (97:3 vol %) solvent (25 g L^{-1}); PCDTBT:$PC_{70}BM$ and PCBTDPP:$PC_{70}BM$ solutions (20 g L^{-1}) were spin-coated from 1,2-diclorobenzene solvent. All polymer:C_{70} blends were dissolved in 1,2-dichlorobenzene (28−30 g L^{-1} for PTB7:C_{70} and PCBTDPP:C_{70} blends, 12−17 g L^{-1}, for PCDTBT:C_{70} blends, depending on the donor/acceptor weight ratio). Then, the samples were transferred to an Ar-filled glovebox, where the device structure was completed with the thermal evaporation of a Ca/Al (20/80 nm) top electrode at the base pressure of 3×10^{-6} mbar. The device active area, defined by the shadow mask used for the cathode deposition, was 8 mm^2. For a better comparison of the cells made of the same donor, the active layers were prepared with the same thickness, 100 and 70 nm for PTB7-based cells and PCDTBT-based cells, respectively, measured with a Tencor Alphastep 200 profilometer.

For hole-only devices, ITO/PEDOT:PSS was used as the bottom contact and Au as the top contact, otherwise, for electron-only devices, Al was used as the bottom contact and LiF/Al as the top contact.

Electrical Characterization. The electrical characterization was carried out in glovebox at room temperature. Solar cells were

illuminated by using a solar simulator (SUN 2000 Abet Technologies, AM1.5G) and the light power intensity was calibrated using a certified silicon solar cells. For light-intensity-dependent measurements, a set of quartz neutral filters was used to vary the incident light power. The current–voltage curves were taken with a Keithley 2400 source-measure unit.

Impedance spectroscopy measurements were conducted using an Agilent 4294A impedance analyzer. The impedance measurements were done in $|Z|-\theta$ mode, with the frequency ranging between 40 Hz and 1 MHz, and with an amplitude of the harmonic voltage modulation of 20 mV. A constant dc bias, equivalent to the open-circuit voltage of solar cells, was superimposed to the ac signal. Experimental data were analyzed with the EIS Spectrum Analyzer program (the program is available online at http://www.abc.chemistry.bsu.by/vi/analyser/).[41]

AFM Microscopy. The blend surface morphology was examined by using tapping-mode atomic force microscopy (Veeco, Multimode IIID Microscope). The blends were deposited onto ITO/PEDOT:PSS substrate by using the same conditions used for the preparation of the related solar cells.

Optical Microscopy. The active blend films were also examined by using standard light microscopy (Nikon Eclipse LV150). All images were taken in air and at room temperature.

3. RESULTS AND DISCUSSION

3.1. Photovoltaic Parameters. Solar cells with $PC_{70}BM$ as electron-acceptor were first prepared with both conjugated polymers, PTB7 and PCDTBT (Figure 1), according to optimized procedures already reported in the literature for the active layer deposition and composition.[42,43] In particular, PTB7:$PC_{70}BM$ solar cells were prepared in 1:1.5 weight ratio and deposited from a chlorobenzene solution with 1,8-diiodooctane (3% vol) as additive, while PCDTBT:$PC_{70}BM$ (1:4 w/w) devices were spin-coated from 1,2-dichlorobenze. C_{70}-based solar cells were prepared in different donor to acceptor (D/A) ratios from 1,2-dichlorobenze solutions, and, for a better comparison, with the same thickness of the active layer of the reference cells made with $PC_{70}BM$ (about 100 nm for P7BT-based cells, about 70 nm for PCDTBT-based cells).

The current density–voltage ($J-V$) characteristics of as-cast C_{70}-based solar cells are shown in Figure 2 and compared with those obtained for the reference cells with $PC_{70}BM$, while the extracted photovoltaic parameters are collected in Table 1. The values calculated for the efficiency of the reference cells are in agreement with those reported in previous studies for devices prepared with a comparable architecture,[42,44] with a PCE of 5.73% calculated for PTB7:$PC_{70}BM$ devices and of 4.80% for PCDTBT:$PC_{70}BM$ cells. As shown in Table 1, the replacement of $PC_{70}BM$ with C_{70} led to the decrease of all photovoltaic parameters, with the only exception of the short-circuit current density (J_{sc}) of PCDTBT:C_{70} solar cells. Indeed, differently from PTB7:C_{70} devices, for which a significant reduction of J_{sc} was observed (J_{sc} of 9.08 and 9.21 mA cm^{-2} for the two D/A ratios) compared to the related reference cell (13.34 mA cm^{-2}), the change of the polymer donor resulted in an enhanced short-circuit current for neat-C_{70} devices, with a J_{sc} ranging between 8.50 and 11.66 mA cm^{-2}, to be compared with 8.41 mA cm^{-2} measured for PCDTBT:$PC_{70}BM$ solar cells. Given the same thickness of the blends made with the same electron-donor, the higher molar extinction coefficient of C_{70} compared to $PC_{70}BM$,[26] and the higher molar amount of the acceptor in neat-C_{70} blends (0.952 mmol/g vs 0.787 mmol/g for D/A of 1:4), an enhanced absorption of light is expected for the active layers made of neat C_{70}, leading to the higher J_{sc} observed for PCDTBT:C_{70} solar cells with respect to the PCDTBT:$PC_{70}BM$ ones. As an example, the absorption coefficients of PCDTBT:C_{70} and PCDTBT:$PC_{70}BM$ films, prepared with the same A/D ratio of 1:4 w/w, are compared in Figure SI1, in the Supporting Information. Differently from PCDTBT donor, the short-circuit current decreased upon replacing $PC_{70}BM$ with C_{70} in PTB7-based solar cells, despite the improved absorption of light. The different behavior of J_{sc} in the cells made of the two polymers could be related to a different charge generation ability of the blends, due to a different distribution of the donor/acceptor interface.

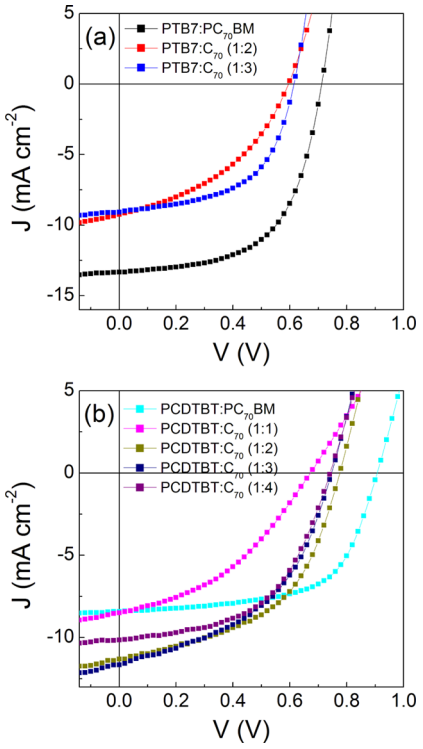

Figure 2. Current density–voltage characteristics under 100 mW cm^{-2} illumination (AM1.5G) for solar cells made of (a) PTB7 or (b) PCDTBT as electron-donor. Donor to acceptor weight ratios for neat-C_{70} cells are indicated in parentheses.

The open-circuit voltage (V_{oc}) decreased from 0.71 and 0.91 V of the reference cells made of PTB7 and PCDTBT, respectively, to values of around 0.6 V for PTB7:C_{70} cells and ranging between 0.67 and 0.78 V in the case of PCDTBT donor. The reduction of V_{oc} upon replacing $PC_{70}BM$ with C_{70} could be explained by the effect of the higher leakage currents observed for cells made of neat-C_{70} (Supporting Information Figure SI2), as well as by the different electron affinities of the electron-acceptors.[45−47] Also, the fill factor (FF) was found to decrease for all C_{70}-based solar cells, irrespective of the donor and of the D/A ratio, indicating higher losses for charge recombination, though also FF is affected by leakage paths. FF values in the range 0.41−0.55 were achieved for PTB7:C_{70} solar cells and between 0.40 and 0.53 for PCDTBT:C_{70} devices, against 0.59 and 0.62 calculated for the respective reference cells. Nevertheless, despite the loss of efficiency of solar cells made with C_{70}, good performances were obtained with PCDTBT donor at high fullerene contents. The photovoltaic parameters of PCDTBT:C_{70} cells for a fullerene content between 66% and 80% by weight were found to be close enough, with a variation of PCE of around 10% (Table 1). Differently, a meaningful reduction of performance was

Table 1. Photovoltaic Parameters at 100 mW cm^{-2} (AM1.5G) of Best-Efficiency Solar Cells[a]

active layer	D:A [w/w]	J_{sc} [mA cm^{-2}]	V_{OC} [V]	FF	PCE [%]
PTB7:$PC_{70}BM$	1:1.5	13.34 (12.82 ± 0.73)	0.71 (0.71 ± 0.00)	0.59 (0.59 ± 0.01)	5.73 (5.52 ± 0.30)
PTB7:C_{70}	1:2	9.21 (8.78 ± 0.41)	0.59 (0.59 ± 0.00)	0.41 (0.41 ± 0.03)	2.22 (2.13 ± 0.10)
PTB7:C_{70}	1:3	9.08 (8.57 ± 0.44)	0.61 (0.61 ± 0.00)	0.55 (0.52 ± 0.30)	3.17 (2.80 ± 0.28)
PCDTBT:$PC_{70}BM$	1:4	8.41 (8.40 ± 0.01)	0.91 (0.90 ± 0.01)	0.62 (0.60 ± 0.14)	4.80 (4.56 ± 0.20)
PCDTBT:C_{70}	1:1	8.50 (7.95 ± 0.41)	0.67 (0.66 ± 0.01)	0.40 (0.40 ± 0.08)	2.30 (2.04 ± 0.19)
PCDTBT:C_{70}	1:2	11.31 (10.72 ± 0.42)	0.78 (0.77 ± 0.01)	0.50 (0.49 ± 0.08)	4.44 (4.13 ± 0.23)
PCDTBT:C_{70}	1:3	11.66 (10.51 ± 1.63)	0.75 (0.74 ± 0.01)	0.47 (0.43 ± 0.30)	4.09 (3.88 ± 0.29)
PCDTBT:C_{70}	1:4	10.15 (9.79 ± 0.28)	0.74 (0.73 ± 0.01)	0.53 (0.52 ± 0.10)	4.02 (3.79 ± 0.19)

[a]Mean values (of 4 devices) and standard deviations are reported in brackets.

observed with 50% by weight of fullerene, suggesting a poor C_{70} network formation for that blend composition. The best performance was obtained for devices prepared with 1:2 D/A ratio, which showed a J_{sc} of 11.31 mA cm^{-2}, V_{oc} = 0.78 V, and FF of 50%, resulting in a PCE of 4.44%, reduced by 7.5% with respect to 4.80% calculated for PCDCTBT:$PC_{70}BM$ reference cell. The peak efficiency for the fullerene content of 66% is consistent with a higher light absorption ability of the blend richest in the conjugated polymer (the main absorber).

To our knowledge, this efficiency value is the record for BHJ polymer solar cells made of neat-fullerenes. On the contrary, for the best PTB7:C_{70} solar cells (1:3 D/A ratio) a reduction of PCE of about 45% was observed by replacing $PC_{70}BM$ with neat-C_{70}.

3.2. Analysis of Photocurrents. In order to investigate the loss mechanisms in the cells made of neat-C_{70}, the behavior of photocurrents was analyzed as a function of voltage at different values of the light power intensity (P_{in}) and compared with that observed for the reference cells. The trend of the neat photocurrent J_{ph}, obtained as the difference between the current under illumination and that flowing in the dark, is plotted in Figures 3 and 4 versus the effective voltage V_0-V for PTB7 and PCDTBT-based solar cells, respectively. V_0 is the compensation voltage; that is, the voltage at which J_{ph} is zero, and V the applied voltage.[48] For PTB7:$PC_{70}BM$ solar cells, J_{ph} quickly saturates, showing a nearly constant value with the effective voltage. In these devices, charge carriers are efficiently collected at the electrodes with no recombination losses, even at low effective voltages, relevant for solar cell operation. Differently, a voltage-dependent behavior of J_{ph} was observed for PCDCTB:$PC_{70}BM$ solar cells (Figure 4a), with the saturation reached at an effective voltage of around 0.3 V independently of P_{in} and with a linear trend of J_{ph} with P_{in} at low V_0-V. It is worth noting that in all cases J_{ph} is not significantly limited at short-circuit conditions (SC, indicated by arrows in Figures 3 and 4), indicating that the built-in voltage is enough to sweep charge carriers out of the cells before they recombine. This was also confirmed by the nearly linear trend of J_{sc} with P_{in} observed for all solar cells (as shown in Supporting Information Figure SI3). Differently, at lower fields, as at the maximum power point (M_{PP}, indicated by arrows in Figures 3 and 4), recombination losses were observed for all cells made of neat-C_{70} as well as for PCDTBT-based reference cells, reflecting in the lower values of *FF* compared to the recombination-free PTB7:$PC_{70}BM$ devices (Table 1).

The different behavior of J_{ph} in the range of low effective voltage could be attributed to different charge transport properties in the blends made of the two different donors. The mobility of charge carriers in PTB7:$PC_{70}BM$ blend should be high enough to allow the extraction of charges before

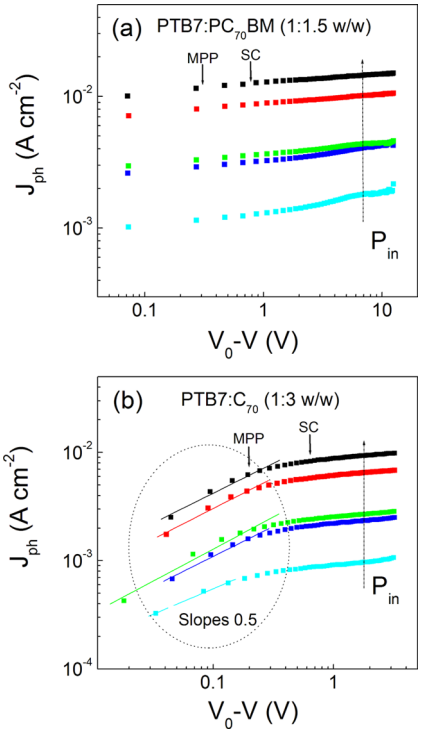

Figure 3. Photocurrent as a function of the effective voltage at different light power intensity (8−100 mW cm^{-2}) for (a) PTB7:$PC_{70}BM$ (1:1.5 w/w) and (b) PTB7:C_{70} (1:3 w/w) solar cells. Short-circuit (SC) and maximum power point (M_{PP}) conditions are indicated by the arrows for the curves obtained at 100 mW cm^{-2}.

recombination even at very low effective voltages, while a lower mobility in PCDTBT:$PC_{70}BM$ solar cells could account for the field-dependent J_{ph} observed at low V_0-V, indicating that the drift length of charge carriers, the path they can cover before recombination, is lower than the blend thickness at those effective voltages and leading to a recombination loss.[49] In effect, the mobility of holes in the donor phase is expected to be higher in PTB7 than in PCDTBT,[50] though charge carrier mobility is extremely dependent on the D/A ratio and the deposition conditions of the blends.

A square-root dependence of J_{ph} with V_0-V was not observed for PCDTBT:$PC_{70}BM$ solar cells in any range of the effective voltage, excluding for these cells space-charge effects or limitation of the photocurrent due to a low $\mu\tau$ product (μ is the mobility of the slowest charge carriers and τ their effective lifetime).[51−53] On the contrary, a square-root regime before saturation was observed for all cells made with neat C_{70}, as shown in Figures 3b and 4b for PTB7:C_{70} (1:3 w/w) and PCDTBT:C_{70} (1:3 w/w), respectively. To discern

dx.doi.org/10.1021/am506394m | ACS Appl. Mater. Interfaces 2014, 6, 21416−21425

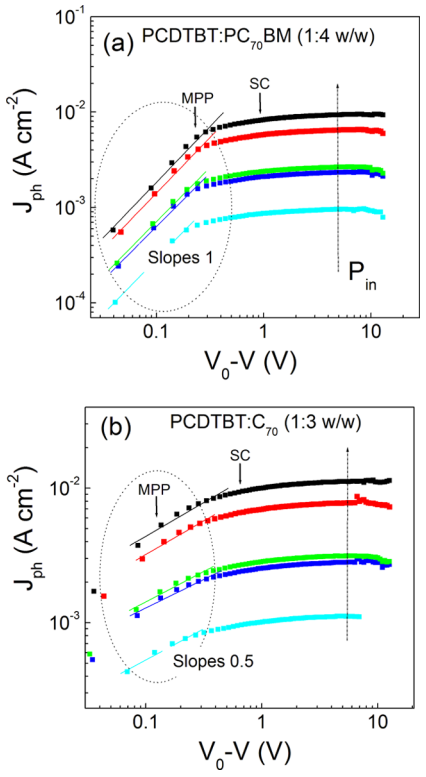

Figure 4. Photocurrent as a function of the effective voltage at different light power intensity (8−100 mW cm^{-2}) for (a) PCDTBT:$PC_{70}BM$ (1:4 w/w) and (b) PCDTBT:C_{70} (1:3 w/w) solar cells. Short-circuit (SC) and maximum power point (M_{PP}) conditions are indicated by the arrows for the curves obtained at 100 mW cm^{-2}.

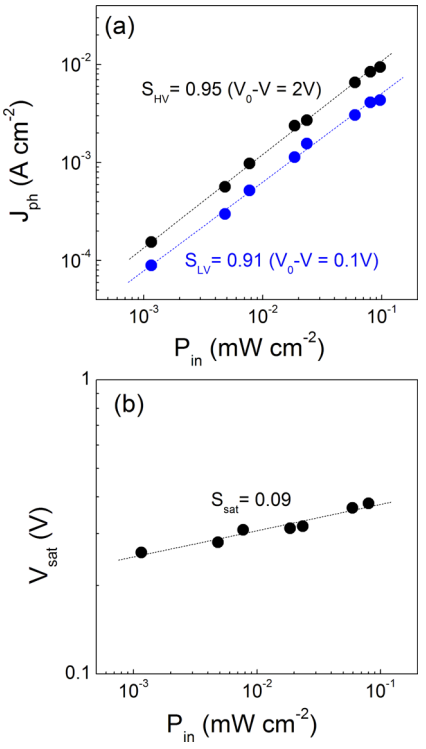

Figure 5. Photocurrent at low and high effective voltage (a) and saturation voltage (b) as a function of light power intensity for PTB7:C_{70} (1:3 w/w) solar cells.

between the two possible limiting processes originating this behavior, space-charge formation or low $\mu\tau$, the trend of J_{ph} and that of the saturation voltage (V_{sat}) was analyzed with P_{in}. V_{sat} is the value of the effective voltage at which the transition from the field-dependent regime to the saturation regime occurs. The results obtained for PTB7:C_{70} (1:3 w/w) solar cells are shown in Figure 5 in bilogarithmic plots. The slope of J_{ph} vs P_{in}, both at high (S_{HV}) and at low effective voltage (S_{LV}) is close to 1. 0.95 and 0.91 were calculated, respectively for S_{HV} and S_{LV}, for PTB7:C_{70} solar cells prepared in 1:3 weight ratio. The $^3/_4$ power dependence of the photocurrent on the incident light was not observed at low P_{in}, indicating that J_{ph} is not limited by the occurrence of space-charge in these cells. The confirmation came from the behavior of V_{sat}, appearing nearly independent of P_{in},[54] so showing a slope with P_{in} (S_{sat}) close to zero (a value of 0.09 was obtained for S_{sat} in the case of PTB7:C_{70} solar cells 1:3 w/w). The same behavior with light intensity was achieved for the other cells made with neat C_{70}, as indicated by the values of S_{HV}, S_{LV}, and S_{sat} collected in Supporting Information Table SI1.

The absence of space-charge formation in the investigated cells could indicate that the mobility of charge carriers is not strongly unbalanced in these cells. To verify this, hole-only and electron-only devices, made with the same blends used for solar cells, were prepared to extract the mobility of charge carriers in the donor and in the acceptor phase by using the space-charge limited current method.[55]

3.3. Charge Carrier Mobility. A good fit of a portion of the $J-V$ characteristics of single-carrier devices (Supporting Information Figure SI4 and SI5) was obtained by using the Mott−Gurney equation modified for the field-dependent mobility:[56]

$$J = \frac{9}{8}\varepsilon\varepsilon_0\mu_0\frac{(V - V_{bi})^2}{L^3}\exp\left(0.89\gamma\sqrt{\frac{V - V_{bi}}{L}}\right) \quad (1)$$

where ε is the relative dielectric constant of the material (3 was assumed), ε_0 the vacuum permittivity, μ_0 the zero-field mobility, V_{bi} the built-in potential resulting from the work function difference of the electrodes, L the film thickness, γ is the field activation factor of mobility, and V is the applied voltage corrected for the voltage drop across the series resistance due to contacts. Extracting the values of μ_0 and γ from the experimental data, the value of μ at any field E can be obtained by using the Poole−Frenkel expression:

$$\mu = \mu_0 \exp(\gamma\sqrt{E}) \quad (2)$$

The series resistance was previously determined in devices with the same geometry and contacts of the single-carrier ones, but without the polymer/fullerene blend. The values of mobility calculated for a field of 5×10^4 V cm^{-1} corresponding to a potential of 0.5 V across a film 100 nm thick and close to the net potential at the maximum power point of the cells (i.e., the difference between the estimated V_{bi} and the voltage at the maximum power point) are summarized in Table 2.

The mobility data of Table 2 indicate a perfectly balanced charge transport for the reference solar cells, with mobilities in agreement with those already reported for the same blends prepared in similar conditions[57] and with the expected higher values for PTB7:$PC_{70}BM$ cells. Upon replacing $PC_{70}BM$ with C_{70}, significant variations of the mobility of negative carriers were not observed, whereas a systematic decrease of the

Table 2. Charge Carrier Mobility Extracted from the *J*–*V* Curves of Single-Carrier Devices[a]

active layer	D/A (w/w)	hole mobility ($cm^2\ V^{-1}\ s^{-1}$)	electron mobility ($cm^2\ V^{-1}\ s^{-1}$)
PTB7:$PC_{70}BM$	1:1.5	3.79×10^{-4}	4.56×10^{-4}
PTB7:C_{70}	1:2	7.29×10^{-5}	1.97×10^{-4}
PTB7:C_{70}	1:3	7.02×10^{-5}	4.25×10^{-4}
PCDTBT:$PC_{70}BM$	1:4	4.48×10^{-5}	3.06×10^{-5}
PCDTBT:C_{70}	1:2	3.66×10^{-6}	1.37×10^{-5}
PCDTBT:C_{70}	1:3	2.77×10^{-6}	1.15×10^{-5}
PCDTBT:C_{70}	1:4	3.17×10^{-6}	3.20×10^{-5}

[a]The mobility values are calculated for an electric field of 5×10^4 V cm^{-1}.

mobility of holes was obtained for both donors. The mobility of positive carriers was reduced by about 5 folds in PTB7:C_{70} blends and by roughly 1 order of magnitude in PCDTBT:C_{70} ones, resulting in charge carrier mobilities not strongly unbalanced, consistent with the absence of space-charge formation in the C_{70}-based solar cells.

The reduction of mobility in the blends made of neat C_{70}, compared to the reference ones prepared with $PC_{70}BM$ as acceptor, could explain the photocurrents limited by a low $\mu\tau$ product. Impedance spectroscopy measurements were performed in order to get further information, in particular, to extract the effective lifetime of charge carriers in the investigated solar cells.

3.4. Impedance Spectra. Impedance spectra were taken under illumination and superimposing on the harmonic voltage modulation a dc bias equivalent to the open-circuit voltage of the device. Under this condition, the photocurrent is canceled by the recombination flux.

Typical impedance spectra obtained for the investigated cells are displayed in Figure 6 for one sun irradiation in the Nyquist representation, with frequency as an implicit variable. The Nyquist plots of PTB7-based devices exhibited a major arc in the investigated frequency range while the impedance spectra of PCDTBT-based cells showed additional features toward higher frequencies (Figure 6b). In both cases, a high quality fit of the experimental data was provided by the equivalent circuit depicted in Figure 6a, as demonstrated by the solid lines through the data points as well as by the low errors associated with the estimated parameters (below 1.5%). The device series resistance is accounted by the resistor R_s in the model circuit of Figure 6a, while R_{rec} represents the recombination resistance, related to the recombination current, and C_μ is the chemical capacitance,[58] due to the accumulation of photogenerated charge carriers and represented in the equivalent circuit by a constant phase element (CPE)[59] for better fittings (with the CPE exponent varying between 0.91 and 1 for the investigated cells). The additional series combination of the resistor R and the constant phase element C, could account for charge trapping phenomena.[60−62] The effective lifetime of charge carriers obtained from R_{rec} and C_μ ($\tau = R_{rec}C_\mu$) was compared with the extraction time (t_{ex}) of slowest charge carriers, holes for solar cells here investigated. The extraction time was estimated considering an average path for carriers to be extracted of $L/2$ and by using the relationship

$$t_{ex} = \frac{L/2}{\mu E} \quad (3)$$

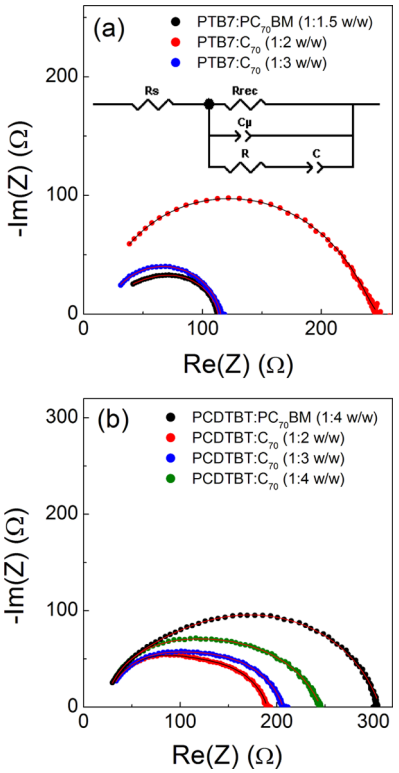

Figure 6. Nyquist plots for solar cells made of (a) PTB7 and (b) PCDTBT polymers under 1 sun irradiation conditions. Lines indicate the fit to the experimental data modeled by the circuit shown in inset.

The values of t_{ex}, obtained from the hole mobilities reported in Table 2 and for $E = 5 \times 10^4$ V cm^{-1} are compared in Figure 7 with the effective lifetimes of charge carriers. For both reference cells τ is longer than t_{ex}, assuring that charge carriers can be efficiently collected at the electrodes before recombination. The situation is reversed when $PC_{70}BM$ is replaced by C_{70}, with t_{ex} much increased due to the lower mobility of charge carriers. As shown in Figure 7, τ did not drastically change by changing the acceptor; however, the product $\mu\tau$, with μ representing the mobility of positive carriers, is significantly reduced in neat-C_{70}-based cells as displayed in Figure 8. The product $\mu\tau$, of the order of 10^{-10} $cm^2\ V^{-1}$ in the reference cells, decreased by 1 order of magnitude, justifying the square-root dependence of the photocurrent on the effective voltage observed for C_{70}-based cells.

3.5. Blend Morphology. Charge transport in the bicontinuous donor/acceptor network of organic solar cells is strictly related to the blend morphology, so the surface morphology of the investigated blends, deposited in the same conditions used for the preparation of solar cells, was characterized by atomic force microscopy (AFM) in tapping mode. The AFM images of PTB7:C_{70} solar cells (Figure 9) revealed an expected highly segregated morphology, reasonably due to the self-aggregation of C_{70} because of its poor solubility.[63] The same very poor dispersion has been found in the P3HT:C_{70} system.[64] On the contrary, the PTB7:$PC_{70}BM$ reference blend showed the formation of a relatively well-organized phase percolation. The formation of large domains with a size of hundreds of nm in PTB7:C_{70} blends could prevent the formation of the continuous interpenetrated donor/acceptor network required for the effective transport of charge carriers, reflecting in the worsening of charge carrier

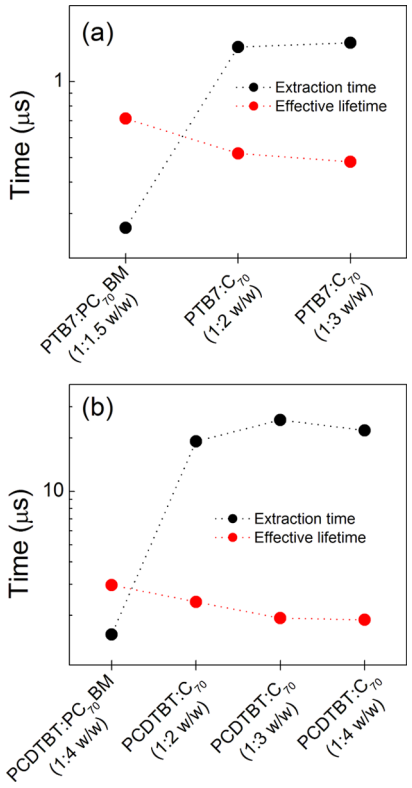

Figure 7. Extraction time and effective lifetime of charge carriers in (a) PTB7-based cells and (b) PCDTBT-based cells.

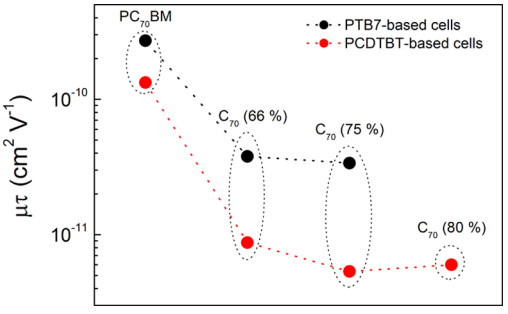

Figure 8. Mobility-lifetime product for PTB7-based cells (black circles) and PCDTBT-based cells (red circles). The percentages by weight of C_{70} are indicated in parentheses.

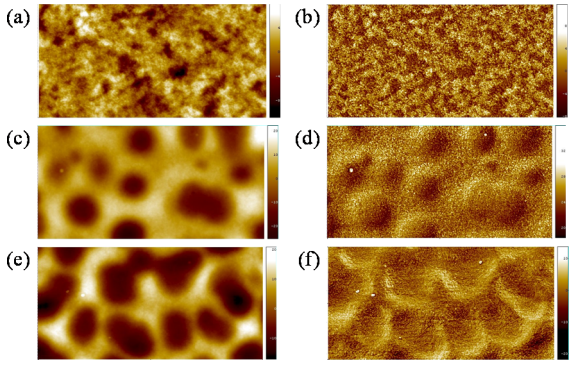

Figure 9. AFM images (2 μm × 1 μm) of PTB7-based blends: (a and b) PTB7:PC_{70}BM (1:1.5 w/w); (c and d) PTB7:C_{70} (1:2 w/w); (e and f) PTB7:C_{70} (1:3 w/w). (a, c, and e) height; (b, d, and f) phase.

mobility. The large-domain morphology of PTB7:C_{70} films was also accomplished by a higher root-mean-square roughness (R_q), compared to the reference blend with PC_{70}BM. The values of R_q, evaluated on a scan area of 2 μm × 1 μm, were 3.10, 5.31, and 7.39 nm for PTB7:PC_{70}BM, PTB7:C_{70} (1:2 w/w) and PTB7:C_{70} (1:3 w/w), respectively.

Surprisingly, by changing the polymer electron donor, the surface morphology observed for the neat-C_{70} blends was very different, as shown in Figure 10, in which the AFM images of

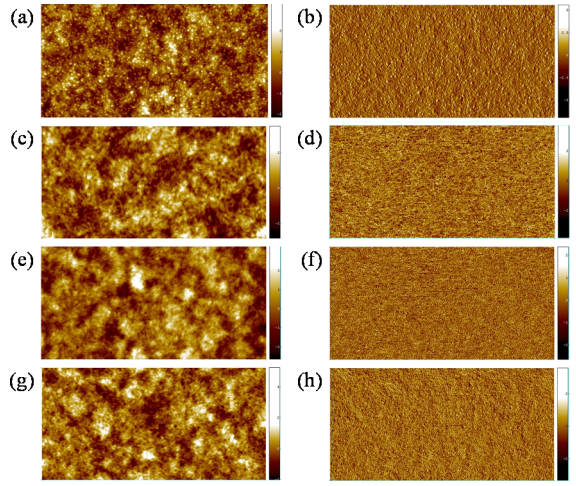

Figure 10. AFM images (2 μm × 1 μm) of PCDTBT-based blends: (a and b) PCDTBT:PC_{70}BM (1:4 w/w); (c and d) PCDTBT:C_{70} (1:1 w/w); (e and f) PCDTBT:C_{70} (1:2 w/w); (g and h) PCDTBT:C_{70} (1:4 w/w). (a, c, e, and g) height; (b, d, f, and h) phase.

PCDCTBT-based blends are compared. Significant differences between PCDTBT:PC_{70}BM and PCDTBT:C_{70} were not revealed, as clearly demonstrated by Figure 10. For all PCDCTBT-based blends, irrespective of the fullerene acceptor, a fine mixing of the two components was achieved. Accordingly, very low and similar R_q values were obtained, ranging between 0.61 and 0.87 nm. The images of Figure 10 indicate that, differently from PTB7, PCDTBT acts as an excellent dispersing medium for C_{70} molecules, enabling low-cost and efficient neat-C_{70} solar cells.

The morphology of the blends is an agreement with the values of the short-circuit current reported in Table 1. Indeed, the reduction of J_{sc} in PTB7-based solar cells by replacing PC_{70}BM with C_{70} can be clearly attributed to the drastic reduction of the extension of the D/A interface, because of the high phase segregation. Differently, the surface morphology of all PCDTBT-based blends is similar, confirming that the enhanced light absorption is the main reason for the higher J_{sc} observed for PCDTBT:C_{70} solar cells, compared to the reference PCDTBT:PC_{70}BM. However, the lower mobility values in the donor phase of PCDTBT:C_{70} blends (Table 2) indicate that the polymer network is not as effective as in the reference PCDTBT:PC_{70}BM mixture in providing adequate pathways for the transport of positive charge carriers.

The unexpected excellent miscibility of PCDTBT:C_{70} blends might be attributed to an interaction between the carbazole unit and fullerene, a mechanism that could favor the dispersion of the acceptor in the polymer matrix, thus limiting the loss of performance of the related cells. Indeed, it has been reported that aromatic amines act as good solvents both for fullerenes[65] and carbon nanotubes,[66] due to a charge-transfer interaction. In

particular, carbazole based-polymers have been indicated as particularly effective in the dispersion of carbon nanotubes,[67,68] thus envisaging a similar property toward fullerenes.

In order to confirm the role of carbazole in the dispersion of fullerene, blends based on another conjugated polymer with the carbazole unit in the molecular structure, poly[N-9′-heptadecanyl-2,7carbazole-*alt*-3,6-bis(thiophen-5-yl)-2,5-dioctyl-2,5-dihydropyrrolo[3,4]pyrrole-1,4-dione][69] (PCBTDPP, Figure 1), were prepared and analyzed. As shown in Figure 11, the

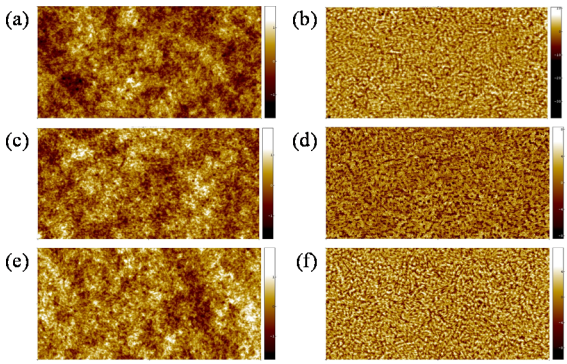

Figure 11. AFM images (2 μm × 1 μm) of PCBTDPP-based blends: (a and b) PCBTDPP:$PC_{70}BM$ (1:3 w/w); (c and d) PCBTDPP:C_{70} (1:3 w/w); (e and f) PCBTDPP:C_{70} (1:2 w/w). (a, c, and e) height; (b, d, and f) phase.

AFM images of PCBTDPP:C_{70} films are indiscernible from that of the reference PCBTDPP:$PC_{70}BM$ blend. As for PCDTBT:C_{70} blends, a finely mixed and smooth surface morphology was observed, with a R_q ranging between 0.39 and 0.55 nm. These results further strengthen the hypothesis of the role of carbazole in determining the morphology of polymer/C_{70} blends. Accordingly, also for solar cells made of PCBTDPP:C_{70} active layers a restrained loss of efficiency was achieved with respect to PCBTDPP:$PC_{70}BM$ reference devices (Supporting Information Figure SI6).

A further confirmation of the key role of carbazole, came from the morphology of blends made of poly[(9,9-bis(2-ethylhexyl)fluorenyl-2,7-diyl-*alt*-5,5-(4′,7′-di-2-thienyl-2′,1′,3′-benzothiadiazole)] (PFDTBT, Figure 1) and C_{70} or $PC_{70}BM$. Indeed, PFDTBT and PCDTBT just differ for the presence of fluorenyl moieties in the polymer backbone in place of the carbazole repeating units. The surface morphology of PFDTBT:C_{70} blends appeared very dissimilar from point to point, as observed by AFM. For these films, the macroscale images (Supporting Information Figure SI7), taken with an optical miscoscope, can better account for the extremely segregated morphology, with the formation of large fullerene aggregates of tens of μm. For comparison, the macroscale images of PCDTBT- and PCBTDPP-based blends are also reported in Supporting Information Figure SI7. Supporting Information Figure SI8 shows the C_{70} aggregates surrounded by the donor (or the donor/acceptor blend) as observed by AFM, which are especially evident in the topographic images.

4. CONCLUSION

The performance of solar cells made of PTB7 or PCDTBT as donors and neat-C_{70} as acceptor are mainly limited by the charge transport properties in the blends, compared to the reference cells made of $PC_{70}BM$. Upon replacing $PC_{70}BM$ with C_{70}, the mobility of positive carriers in the donor phase is roughly reduced by 1 order of magnitude, while that of electrons is only slightly modified. Though a strong unbalanced transport was not observed in C_{70}-based cells, preventing space-charge formation, a limitation of the photocurrent due to a low $\mu\tau$ product was systematically observed, independently of the polymer donor and the D/A ratio.

The modified charge transport properties in the C_{70}-based cells were determined by the blend morphology, affected by the replacement of the acceptor. A highly segregated morphology was observed for PTB7:C_{70} solar cells, with the formation of large domains with a size of hundreds of nm. Given the worse mobility of holes in these blends, poorly interconnected domains in the donor phase can be hypothesized. Differently, PCDTBT was an excellent dispersant for C_{70} and the comparison of the surface morphology of PCDTBT:C_{70} and PCDTBT:$PC_{70}BM$ blends did not reveal significant differences, at least on the scale explored by the AFM. However, despite the relevant difference of the surface morphology of C_{70}-based blends made of the two polymers, a consistent reduction of the hole mobility was also observed for PCDTBT:C_{70} solar cells, indicating that the D/A mixing is not so effective in the formation of the bicontinuous donor and acceptor domains required for efficient charge transport.

Nevertheless, thanks to the enhanced light absorption of the blends made of neat-C_{70}, PCDTBT:C_{70} solar cells underwent a limited loss of efficiency (7.5%), compared to the reference PCDTBT:$PC_{70}BM$. A PCE of 4.44% was reached, a record for BHJ polymer devices with unfunctionalized fullerenes, demonstrating that high efficiency solar cells made of cheaper neat-fullerene are possible if the right donor is selected.

The excellent miscibility of PCDTBT:C_{70} blends was attributed to an interaction between fullerene and the carbazole unit of PCDTBT (which would act as a true interfacial agent), confirmed by the behavior of neat-C_{70} blends made with PCBTDPP, also containing carbazole in its molecular structure. Differently, blends made of carbazole-free polymers, PTB7and PFDTBT, showed the expected highly segregated morphology when neat-C_{70} was used as acceptor, as already observed also for P3HT:C_{70} active layers.

In summary, the results here reported indicate that efficient bulk-heterojunction solar cells are possible with low-cost unfunctionalized fullerenes and carbazole-containing conjugated polymers, a strategy that would further reduce the environmental footprint of this already "green" technology.

■ ASSOCIATED CONTENT

Supporting Information

Absorption coefficients of PCDTBT:PC70BM and PCDTBT:C70 films; current density−voltage characteristics in the dark of solar cells; short-circuit current as a function of the incident light power intensity; slopes of J_{ph} vs P_{in} and V_{sat} vs P_{in}; current−voltage curves of one-carrier-only PTB7- and PCDTBT based devices; current density−voltage characteristics for PCBTDPP-based solar cells; optical images of PFDTBT, PCBTDPP, and PCDTBT based blends. This material is available free of charge via the Internet at http://pubs.acs.org.

■ AUTHOR INFORMATION

Corresponding Authors

*E-mail: riccardo.po@eni.com.
*E-mail: nadia.camaioni@isof.cnr.it.

Notes

The authors declare no competing financial interest.

■ ACKNOWLEDGMENTS

This work was supported by ENI S.p.A. (contract no. 4700007315).

■ REFERENCES

(1) Liao, S.-H.; Jhuo, H.-J.; Cheng, Y.-S.; Chen, S. A. Fullerene Derivative-Doped Zinc Oxide Nanofilm as the Cathode of Inverted Polymer Solar Cells with Low-Bandgap Polymer (PTB7-Th) for High Performance. *Adv. Mater.* **2013**, *25*, 4766−4771.

(2) He, Z.; Zhong, C.; Su, S.; Xu, M.; Wu, H.; Cao, Y. Enhanced Power-Conversion Efficiency in Polymer Solar Cells Using an Inverted Device Structure. *Nat. Photonics* **2012**, *6*, 591−595.

(3) You, J.; Dou, L.; Yoshimura, K.; Kato, T.; Ohya, K.; Moriarty, T.; Emery, K.; Chen, C. C.; Gao, J.; Li, G.; Yang, Y. A Polymer Tandem Solar Cell with 10.6% Power Conversion Efficiency. *Nat. Commun.* **2013**, *4*, 1446.

(4) Guo, X. G.; Zhou, N. J.; Lou, S. J.; Smith, J.; Tice, D. B.; Hennek, J. W.; Ortiz, R. P.; Navarrete, J. T. L.; Li, S. Y.; Strzalka, J.; Chen, L. X.; Chang, R. P. H.; Facchetti, A.; Marks, T. J. Polymer Solar Cells with Enhanced Fill Factors. *Nat. Photonics* **2013**, *7*, 825−833.

(5) Gendron, D.; Leclerc, M. New Conjugated Polymers for Plastic Solar Cells. *Energy Environ. Sci.* **2011**, *4*, 1225−1237.

(6) Son, H. J.; Carsten, B.; Jung, I. H.; Yu, L. Overcoming Efficiency Challenges in Organic Solar Cells: Rational Development of Conjugated Polymers. *Energy Environ. Sci.* **2012**, *5*, 8158−8170.

(7) Li, Y. Molecular Design of Photovoltaic Materials for Polymer Solar Cells: Toward Suitable Electronic Energy Levels and Broad Absorption. *Acc. Chem. Res.* **2012**, *45*, 723−733.

(8) Burkhart, B.; Thompson, B. C. Solution-Processed Donors. In *Organic Solar Cells. Fundamentals, Devices, and Upscaling*; Rand, B. P.; Richter, H., Eds.; Pan Stanford Publishing: Singapore, 2014.

(9) He, Y.; Hong, W.; Li, Y. New Building Blocks for π-Conjugated Polymer Semiconductors for Organic Thin Film Transistors and Photovoltaics. *J. Mater. Chem. C* **2014**, *2*, 8651−8661.

(10) Huang, Y.; Kramer, E. J.; Heeger, A. J.; Bazan, G. C. Bulk Heterojunction Solar Cells: Morphology and Performance Relationships. *Chem. Rev.* **2014**, *114*, 7006−7043.

(11) Po, R.; Carbonera, C.; Bernardi, A.; Camaioni, N. The Role of Buffer Layers in Polymer Solar Cells. *Energy Environ. Sci.* **2011**, *4*, 285−310.

(12) Po, R.; Carbonera, C.; Bernardi, A.; Tinti, F.; Camaioni, N. Polymer- and Carbon-Based Electrodes for Polymer Solar Cells: Toward Low-Cost, Continuous Fabrication over Large Area. *Sol. Energy Mater. Sol. Cells* **2012**, *100*, 97−114.

(13) Sonar, P.; Lin, J.P. F.; Chan, K. L. Organic Non-Fullerene Acceptors for Organic Photovoltaics. *Energy Environ. Sci.* **2011**, *4*, 1558−1574.

(14) Guo, X.; Cui, C.; Zhang, M.; Huo, L.; Huang, Y.; Hou, J.; Li, Y. High Efficiency Polymer Solar Cells Based on Poly(3-hexylthiophene)/Indene-C70 Bisadduct with Solvent Additive. *Energy Environ. Sci.* **2012**, *5*, 7943−7949.

(15) Lai, Y.-Y.; Cheng, Y.-J.; Hsu, C.-S. Applications of Functional Fullerene Materials in Polymer Solar Cells. *Energy Environ. Sci.* **2014**, *7*, 1866−1883.

(16) Li, C.-Z.; Yip, H.-L.; Jen, A. K.-Y. Functional Fullerenes for Organic Photovoltaics. *J. Mater. Chem.* **2012**, *22*, 4161−4177.

(17) He, Y.; Li, Y. Fullerene Derivative Acceptors for High Performance Polymer Solar Cells. *Phys. Chem. Chem. Phys.* **2011**, *13*, 1970−1983.

(18) Marzano, G.; Cascia, C. V.; Babudri, F.; Bianchi, G.; Pellegrino, A.; Po, R.; Farinola, G. M. Organometallic Approaches to Conjugated Polymers for Plastic Solar Cells: from Laboratory Synthesis to Industrial Production. *Eur. J. Org. Chem.* **2014**, *30*, 6583−6614.

(19) Espinosa, N.; Hosel, M.; Jorgensen, M.; Krebs, F. C. Large Scale Deployment of Polymer Solar Cells on Land, on Sea and in the Air. *Energy Environ. Sci.* **2014**, *7*, 855−866.

(20) Krebs, F. C.; Fyenbo, J.; Tanenbaum, D. M.; Gevorgyan, S. A.; Andriessen, R.; van Remoortere, B.; Galagan, Y.; Jørgensen, M. The OE-A OPV Demonstrator Anno Domini 2011. *Energy Environ. Sci.* **2011**, *4*, 4116−4123.

(21) Machui, F.; Hösel, M.; Li, N.; Spyropoulos, G. D.; Ameri, T.; Søndergaard, R. R.; Jørgensen, M.; Scheel, A.; Gaiser, D.; Kreul, K.; Lenssen, D.; Legros, M.; Lemaitre, N.; Vilkman, M.; Välimäki, M.; Nordman, S.; Brabec, C. J.; Krebs, F. C. Cost Analysis of Roll-to-Roll Fabricated ITO Free Single and Tandem Organic Solar Modules Based on Data from Manufacture. *Energy Environ. Sci.* **2014**, *7*, 2792−2801.

(22) Osedach, T. P.; Andrew, T. L.; Bulovic, V. Effect of Synthetic Accessibility on the Commercial Viability of Organic Photovoltaics. *Energy Environ. Sci.* **2013**, *6*, 711−718.

(23) Roncali, J.; Leriche, P.; Blanchard, P. Molecular Materials for Organic Photovoltaics: Small is Beautiful. *Adv. Mater.* **2014**, *26*, 3821−3838.

(24) Po, R.; Bernardi, A.; Calabrese, A.; Carbonera, C.; Corso, G.; Pellegrino, A. From Lab to Fab: How Must the Polymer Solar Cells Materials Design Change? An Industrial Perspective. *Energy Environ. Sci.* **2014**, *7*, 925−943.

(25) www.solarischem.com, accessed on November 2014.

(26) Lin, H.-W.; Chang, J.-H.; Huang, W.-C.; Lin, Y.-T.; Lin, F.; Wong, K.-T.; Wang, H.-F.; Ho, R.-M.; Meng, H.-F. Highly Efficient Organic Solar Cells Using a Solution-Processed Active Layer with a Small Molecule Donor and Pristine Fullerene. *J. Mater. Chem. A* **2014**, *2*, 3709−3714.

(27) Anctil, A.; Babbitt, C. W.; Raffaelle, R. P.; Landi, B. J. Cumulative Energy Demand for Small Molecule and Polymer Photovoltaics. *Prog. Photovoltaics* **2013**, *21*, 1541−1554.

(28) Marcus, Y.; Smith, A. L.; Korobov, M. V.; Mirakyan, A. L.; Avramenko, N. V.; Stukalin, E. B. Solubility of C60 Fullerene. *J. Phys. Chem. B* **2001**, *105*, 2499−2506.

(29) Ruoff, R. S.; Tse, D. S.; Malhotra, R.; Lorents, D. L. Solubility of C60 Fullerene in a Variety of Solvents. *J. Phys. Chem.* **1993**, *97*, 3379−3383.

(30) Rait, S.; Kashyap, S.; Bhatnagar, P. K.; Mathur, P. C.; Sengupta, S. K.; Kumar, J. Improving Power Conversion Efficiency in Polythiophene/Fullerene-Based Bulk Heterojunction Solar Cells. *Sol. Energy Mater. Sol. Cells* **2007**, *91*, 757−763.

(31) Motaung, D. E.; Malgas, G. F.; Arendse, C. J.; Mavundla, S. E.; Oliphant, C. J.; Knoesen, D. Thermal-Induced Changes on the Properties of Spin-Coated P3HT:C60 Thin Films for Solar Cell Applications. *Sol. Energy Mater. Sol. Cells* **2009**, *93*, 1674−1680.

(32) Tang, H.; Lu, G.; Yang, X. The Role of Morphology Control in Determining the Performance of P3HT/C-70 Bulk Heterojunction Polymer Solar Cells. *IEEE J. Sel. Top. Quantum Electron.* **2010**, *16*, 1725−1731.

(33) Tada, K.; Onoda, M. Poor Man's Green Bulk Heterojunction Photocells: A Chlorine-Free Solvent for Poly(3-hexylthiophene)/C60 Composites. *Sol. Energy Mater. Sol. Cells* **2012**, *100*, 246−250.

(34) Chan, S.-H.; Lai, C.-S.; Chen, H.-L.; Ting, C.; Chen, C.-P. Highly Efficient P3HT: C60 Solar Cell Free of Annealing Process. *Macromolecules* **2011**, *44*, 8886−8891.

(35) Lu, G.; Li, L.; Yang, X. Creating a Uniform Distribution of Fullerene C60 Nanorods in a Polymer Matrix and its Photovoltaic Applications. *Small* **2008**, *4*, 601−606.

(36) Tada, K. Yet Another Poor Man's Green Bulk Heterojunction Photocells: Annealing Effect and Film Composition Dependence of Photovoltaic Devices using Poly(3-hexylthiophene):C70 Composites Prepared with Chlorine-Free Solvent. *Sol. Energy Mater. Sol. Cells* **2013**, *108*, 82−86.

(37) Tada, K. Bulk Heterojunction Photocells Utilizing Neat C70 and Low Energy-Gap Polymer Prepared with Halogen-Free Solvent. *Sol. Energy Mater. Sol. Cells* **2013**, *117*, 194−197.

(38) Tada, K. Interplay Between Annealing Temperature and Optimum Composition and Fullerene Aggregation Effects in Bulk Heterojunction Photocells Based on Poly(3-hexylthiophene) and Unmodified C60. *Sol. Energy Mater. Sol. Cells* **2014**, *120*, 136−142.
(39) Tada, K. Effect of Conjugated Polyelectrolyte Interlayer at Cathode in Bulk Heterojunction Photocells Based on Neat C70 and Low-Energy-Gap Polymer Prepared with Halogen-Free Solvent. *Appl. Phys. Express* **2014**, *7*, 051601.
(40) Bonoldi, L.; Calabrese, A.; Pellegrino, A.; Po, R.; Perin, N.; Spera, S.; Tacca, A. Optical and Electronic Properties of Thiophene, Fluorene, Benzothiadiazole Random Copolymers for Photovoltaic Applications. *J. Mater. Sci.* **2011**, *46*, 3960−3968.
(41) Bondarenko, A. S.; Ragoisha, G. A. In *Progress in Chemometrics Research*; Pomerantsev, A. L., Ed.; Nova Science Publishers: New York, 2005.
(42) Collins, B. A.; Li, Z.; Tumbleston, J. R.; Gann, E.; McNeill, C. R.; Ade, H. Absolute Measurement of Domain Composition and Nanoscale Size Distribution Explains Performance in PTB7:PC71BM Solar Cells. *Adv. Energy Mater.* **2013**, *3*, 65−74.
(43) Namkoong, G.; Kong, J.; Samson, M.; Hwang, I.-W.; Lee, K. Active Layer Thickness Effect on the Recombination Process of PCDTBT:PC71BM Organic Solar Cells. *Org. Electron.* **2013**, *14*, 74−79.
(44) Sun, K.; Zhao, B.; Muregesan, V.; Kumar, A.; Zeng, K.; Subbiah, J.; Wong, W. W. H.; Jones, D. J.; Ouyang, J. High-Performance Polymer Solar Cells with a Conjugated Zwitterion by Solution Processing or Thermal Deposition as the Electron-Collection Interlayer. *J. Mater. Chem.* **2012**, *22*, 24155−24165.
(45) Scharber, M. C.; Mühlbacher, D.; Koppe, M.; Denk, P.; Waldauf, C.; Heeger, A. J.; Brabec, C. J. Design Rules for Donors in Bulk-Heterojunction Solar Cells—Towards 10% Energy-Conversion Efficiency. *Adv. Mater.* **2006**, *18*, 789−794.
(46) Kronholm, D. F.; Hummelen, J. C. In *Organic Photovoltaics: Materials, Device Physics, and Manufacturing Technologies*, 1st ed.; Brabec, C. J., Dyakonov, V., Scherf, U. , Eds.; Wiley-VCH: Weinheim, 2008.
(47) Derbal-Habak, H.; Bergeret, C.; Cousseau, J.; Simon, J. J.; Escoubas, L.; Nunzi, J.-M. New Fullerene Derivatives for the Photovoltaic Application. *J. Photonics Energy* **2011**, *1*, 011120.
(48) Mihailetchi, V. D.; Koster, L. J. A.; Hummelen, J. C.; Blom, P. W. M. Photocurrent Generation in Polymer−Fullerene Bulk Heterojunctions. *Phys. Rev. Lett.* **2004**, *93*, 216601.
(49) Goodman, A. M.; Rose, A. Double Extraction of Uniformly Generated Electron-Hole Pairs from Insulators with Noninjecting Contacts. *J. Appl. Phys.* **1971**, *42*, 2823−2830.
(50) Wang, T.; Pearson, A. J.; Dunbar, A. D. F.; Staniec, P. A.; Watters, D. C.; Yi, H.; Ryan, A. J.; Jones, R. A. L.; Iraqi, A.; Lidzey, D. G. Correlating Structure with Function in Thermally Annealed PCDTBT: PC70BM Photovoltaic Blends. *Adv. Funct. Mater.* **2012**, *22*, 1399−1408.
(51) Blom, P. W. M.; Mihailetchi, V. D.; Koster, L. J. A.; Markov, D. E. Device Physics of Polymer/Fullerene Bulk Heterojunction Solar Cells. *Adv. Mater.* **2007**, *19*, 1551−1566.
(52) Mihailetchi, V. D.; Wildeman, J.; Blom, P. W. M. Space-Charge Limited Photocurrent. *Phys. Rev. Lett.* **2005**, *94*, 126602.
(53) Lenes, M.; Morana, M.; Brabec, C. J.; Blom, P. W. M. Recombination-Limited Photocurrents in Low Bandgap Polymer/Fullerene Solar Cells. *Adv. Funct. Mater.* **2009**, *19*, 1106−1111.
(54) Azimi, H.; Senes, A.; Scharber, M. C.; Hingerl, K.; Brabec, C. J. Charge Transport and Recombination in Low-Bandgap Bulk Heterojunction Solar Cell using Bis-adduct Fullerene. *Adv. Energy Mater.* **2011**, *1*, 1162−1168.
(55) Lampert, M. A.; Mark, P. In *Current Injection in Solids*; Academic Press: New York, 1970.
(56) Murgatroyd, P. N. Theory of Space-Charge-Limited Current Enhanced by Frenkel Effect. *J. Phys. D: Appl. Phys.* **1970**, *3*, 151−156.
(57) He, Z.; Zhoung, C.; Huang, X.; Wong, W.-Y.; Wu, H.; Chen, L.; Su, S.; Cao, Y. Simultaneous Enhancement of Open-Circuit Voltage, Short-Circuit Current Density, and Fill Factor in Polymer Solar Cells. *Adv. Mater.* **2011**, *23*, 4636−4643.
(58) Garcia-Belmonte, G.; Boix, P. P.; Bisquert, J.; Sessolo, M.; Bolink, H. J. Simultaneous Determination of Carrier Lifetime and Electron Density-of-States in P3HT:PCBM Organic Solar Cells Under Illumination by Impedance Spectroscopy. *Sol. Energy Mater. Sol. Cells* **2010**, *94*, 366−375.
(59) Raistrick, I. D.; Macdonald, J. R.; Franceschetti, D. R. In *Impedance Spectroscopy*, 1st ed.; Macdonald, J. R., Ed.; Wiley-Interscience: New York, 1987.
(60) Mani, A.; Huisman, C.; Goossens, A.; Schoonman, J. Mott−Schottky Analysis and Impedance Spectroscopy of TiO_2/6T and ZnO/6T Devices. *J. Phys. Chem. B* **2008**, *112*, 10086−10091.
(61) Leong, W. L.; Cowan, S. R.; Heeger, A. J. Differential Resistance Analysis of Charge Carrier Losses in Organic Bulk Heterojunction Solar Cells: Observing the Transition from Bimolecular to Trap-Assisted Recombination and Quantifying the Order of Recombination. *Adv. Energy Mater.* **2011**, *1*, 517−522.
(62) Zhou, H.; Zhang, Y.; Seifter, J.; Collins, S. D.; Luo, C.; Bazan, G. C.; Nguyen, T.-Q.; Heeger, A. J. High-Efficiency Polymer Solar Cells Enhanced by Solvent Treatment. *Adv. Mater.* **2013**, *25*, 1646−1652.
(63) Sivaraman, N.; Dhamodaran, R.; Kaliappan, I.; Srinivasan, T. G.; Vasudeva Rao, P. R. P.; Mathews, C. K. C. Solubility of C70 in Organic Solvents. *Fullerene Sci. Technol.* **1994**, *2*, 233−246.
(64) Cominetti, A.; Pellegrino, A.; Longo, L.; Po, R.; Tacca, A.; Carbonera, C.; Salvalaggio, M. Polymer Solar Cells Based on Fullerene−Pyrene Acceptor Systems *Mater. Chem. Phys.* submitted.
(65) Wang, Y. Photophysical Properties of Fullerenes and Fullerene/N,N-Diethylaniline Charge-Transfer Complexes. *J. Phys. Chem.* **1992**, *96*, 764−767.
(66) Sun, Y.; Wilson, S. R.; Schuster, D. I. High Dissolution and Strong Light Emission of Carbon Nanotubes in Aromatic Amine Solvents. *J. Am. Chem. Soc.* **2001**, *123*, 5348−5349.
(67) Cadek, M.; Coleman, J. N.; Barron, V.; Hedicke, K.; Blau, W. J. Morphological and Mechanical Properties of Carbon-Nanotube-Reinforced Semicrystalline and Amorphous Polymer Composites. *Appl. Phys. Lett.* **2002**, *81*, 5123−5125.
(68) Lemasson, F. A.; Strunk, T.; Gerstel, P.; Hennrich, F.; Lebedkin, S.; Barner-Kowollik, C.; Wenzel, W.; Kappes, M. M.; Mayor, M. Selective Dispersion of Single-Walled Carbon Nanotubes with Specific Chiral Indices by Poly(N-decyl-2,7-carbazole). *J. Am. Chem. Soc.* **2011**, *133*, 652−655.
(69) Zou, Y.; Gendron, D.; Badrou-Aïch, R.; Najari, A.; Tao, Y.; Leclerc, M. A High-Mobility Low-Bandgap Poly(2,7-carbazole) Derivative for Photovoltaic Applications. *Macromolecules* **2009**, *42*, 2891−2894.